Available online at www.sciencedirect.com

SciVerse ScienceDirect

Ceramics International 39 (2013) 4293–4298

CERAMICS INTERNATIONAL

www.elsevier.com/locate/ceramint

Characterization of electrochromic tungsten oxide film from electrochemical anodized RF-sputtered tungsten films

Chun-Kai Wang[a], Chung-Kwei Lin[b], Ching-Lin Wu[a], Sanjaya Brahma[c], Sheng-Chang Wang[d], Jow-Lay Huang[a,c,e,f,*]

[a]Department of Materials Science and Engineering, National Cheng Kung University, Tainan, Taiwan
[b]School of Dental Technology, College of Oral Medicine, Taipei Medical University, Taipei, Taiwan
[c]Center for Micro/Nano Science and Technology, National Cheng Kung University, Tainan, Taiwan
[d]Department of Mechanical Engineering, Southern Taiwan University, Tainan, Taiwan
[e]Research Center for Energy Technology and Strategy, National Cheng Kung University, Tainan, Taiwan
[f]Department of Chemical and Materials Engineering, National University of Kaohsiung, Kaohsiung, Taiwan

Received 8 September 2012; received in revised form 6 November 2012; accepted 6 November 2012
Available online 13 November 2012

Abstract

Tungsten oxide (WO_3) films prepared by annealing electrochemically anodized metallic tungsten (W) films deposited by radio-frequency sputtering were characterized. Tungsten oxide films of various morphology, crystallinity, and porosity can be prepared by carefully altering the anodization time (20–50 min) and annealing temperature (450–550 °C). The film obtained after 40 min of anodization, and that annealed at 500 °C shows the best electrochromic performance with optical modulation of 43.6% and coloration efficiency of 42.8 cm^2/C. The effects of anodization time and annealing temperature on microstructure and electrochromic properties were addressed.

Keywords: Tungsten oxide film; Electrochemical anodization; Electrochromism

1. Introduction

Electrochromism refers a reversible and persistent change of optical properties of a material induced by the application of an external voltage, and is an active area of basic and applied research in last few decades. Tungsten trioxide (WO_3) has received considerable attention among researchers because of its versatility in applications in electrochromic (EC) devices [1–9], EC displays [10–12], smart windows [13–16], self-dimming rear mirrors [17] and other applications such as gas sensors [18,19], photocatalytic systems [20], photovoltaic devices and photo-electrochemical devices [21,22]. Many transition metal oxides such as tungsten, nickel, iridium, vanadium, titanium, cobalt and molybdenum, show EC properties [23, 24]. However, WO_3 is a key material of choice because of its multiple valence states, high coloration efficiency, good stability and its application in EC device has been reviewed extensively [5,25–27].

It is well known that the electrochromism of WO_3 is caused by the double injection/extraction of electrons and ions, which modify the band structure of WO_3 and change the film color. There is a significant variation in the EC property with the variation in the crystallinity of WO_3. For example, crystalline and ordered WO_3 structures may be considered to show better device property [4,9], and in nanostructured form having large surface area and porous structure, it is expected to show a significantly improved EC property [28]. Apart from that the electrochromic properties of WO_3 films are influenced by microstructure, porosity, chemical composition, as well as the synthesis process [29]. Various synthesis strategies have been realized for the fabrication of WO_3 thin films such as sputtering [30], pulsed laser deposition [31], thermal evaporation [32], chemical vapor deposition [4,33], electrodeposition [2],

*Corresponding author at: Department of Materials Science and Engineering, National Cheng Kung University, Tainan, Taiwan.
E-mail address: jlh888@mail.ncku.edu.tw (J.-L. Huang).

0272-8842/$ - see front matter © 2012 Elsevier Ltd and Techna Group S.r.l. All rights reserved.
http://dx.doi.org/10.1016/j.ceramint.2012.11.010

sol–gel synthesis [34–37], hydrothermal method [38–40] and electrochemical anodization of tungsten foils and films [41–43]. Amongst those methods, electrochemical anodization process is advantageous in producing ordered nanoporous structures having high surface to volume ratio and enhanced electro-optical properties and the anodized surfaces have great potential for the fabrication of optical and electronic devices. Nah et al. [41] prepared porous WO_3 films by anodizing W foil and obtained higher photoelectrochemical current, as compared with sputtered WO_3 film. Watcharenwong et al. [43] described the synthesis of WO_3 by electrochemical anodization in different anodization media and at different applied voltages, showing enhanced photocatalytic activity. Recently, Zhang et al. [8] have prepared porous WO_3 films by electrochemical anodization with direct current (DC)-sputtered W film as the initial material and found improved electrochromic performance. However, the effects of processing parameters on the structure and electrochromic properties remained ambiguous. The present study investigates the effects of anodization time and annealing temperature on the microstructure and electrochromic properties of WO_3 films.

2. Experimental details

The thin film preparation involved a three-step process: (i) deposition of metallic tungsten (W) film on indium tin oxide (ITO) coated glass by radio-frequency (RF) sputtering, (ii) electrochemical anodization of metallic W film, and (iii) annealing of anodized W film. Metallic W films were deposited onto an ITO/glass substrate (15 Ω/sq., AimCore Technology Co., Ltd, Taiwan) by RF magnetron sputtering using a W target (99.95% purity, 2 in. diameter). The vacuum chamber was pumped to a base pressure of $< 2.6 \times 10^{-4}$ Pa and pre-sputtering was performed at 25 W for 10 min to clean the target surface prior to deposition. The W films were deposited at a working pressure of 6.65 Pa with a power of 75 W. During deposition, the substrate was heated to 300 °C and positioned at a distance of 7 cm vertical to the target. Electrochemical anodization was performed using a DC power supply (Agilent 6634B, USA) with an applied voltage of 60 V with a conventional cathode–anode configuration [8,42], where the working electrode was the as-deposited W film and the counter electrode was Pt foil. The anodization duration was varied from 20 to 50 min. After anodization treatment, the as-anodized films were annealed at various temperatures (450, 500, and 550 °C) for 4 h in the ambient atmosphere. The heating/cooling rate was fixed at 5 °C/min. Experiments were carried out by varying the anodization time and annealing temperature to determine their effects on the microstructure and electrochromic properties of WO_3 films. Five WO_3 films, namely TO1, TO2, TO3, TO4, and TO5 (TO—tungsten oxide), were used. Table 1 summarizes the details of the samples and their corresponding processing parameters.

The crystalline structure of as-deposited, as-anodized, and annealed films were examined by X-ray diffraction (XRD, Rigaku Multiflex 2 kW, Japan) with Cu K_α radiation ($\lambda = 1.54$ Å) and Raman spectroscopy (Labram HR, Jobin–Yvon, France) with 633 nm laser as the excitation source. The surface morphology and cross-sectional view of annealed WO_3 films were examined by field-emission scanning electron microscopy (FE-SEM, Hitachi S4800, Japan). The refractive index of WO_3 film was measured by n & k analyzer 1280 (n & k Technology, Inc., USA) and used to calculate the relative density of the film by Lorentz–Lorenz formula [44,45]:

$$\rho_{rel} = \frac{\rho_f}{\rho_b} = \frac{(n_b^2+1)(n_f^2-1)}{(n_b^2-1)(n_f^2+1)}$$

where ρ_{rel} is the relative density, ρ_f is the film density, ρ_b is the bulk density, n_b is the bulk refractive index of WO_3 at 550 nm and is equal to 2.5, and n_f is the refractive index of WO_3 film. The electrochromic properties were investigated by ultraviolet–visible (UV–vis) spectroscopy and a potentiostat. The transmission spectra of bleached and colored states of WO_3 films were examined by a UV–vis spectrophotometer (V650, Jasco, Japan). The coloration/bleaching reactions were performed by applying a step potential of −1/1.5 V for 3 min with a potentiostat (PAR VersaStat II, Princeton Applied Research, USA) in a three-electrode

Table 1
Sample codes and electrochromic properties of WO_3 films fabricated with various anodization times and post-annealing temperatures.

Sample code	Anodization time ($_{min}$)	Annealing temperature (°C)	n_{550}	ρ_{rel} (%)	T_b at 633 nm	T_c at 633 nm	ΔT_{633}	Coloration efficiency ($cm^2\ C^{-1}$)
Variation of annealing temperature (anodization time fixed)								
TO1	40	450	1.53	55.4	66.5	43.8	22.7	40.5
TO2	40	500	1.67	65.2	56.9	13.3	43.6	42.8
TO3	40	550	1.76	70.7	41.2	11.7	29.4	19.1
Variation of anodization time (annealing temperature fixed)								
TO4	20	500	1.84	75.1	36.2	5.6	30.6	31.5
TO5	50	500	1.68	65.8	57.7	29.2	28.5	20.4

T_b and T_c: transmittance values of films at bleached and colored states, respectively.
ΔT_{633}: difference of transmittance between bleached and colored states.

configurations, where the working, counter, and reference electrodes were the WO_3 film, Pt foil, and a saturated Ag/AgCl electrode, respectively. The cyclic voltammograms were obtained in the same electrode configuration in the potential range of -1 to 1.5 V with a scan rate of 50 mV/min. The electrolyte was 1 M $LiClO_4$/propylene carbonate solution.

3. Results and discussion

The as-prepared tungsten film had a metallic sheen and did not show any electrochromic behavior. After anodization, the color of the tungsten oxide film changed to pale brown, showing limited transmittance ($<20\%$) and poor electrochromic performance in the visible range. A similar trend has been previously reported [8].

X-ray diffraction (XRD) was used to investigate the phase formation and crystallographic structure of WO_3 films at various stages (as-deposited, as-anodized, and annealed films) of processing. Fig. 1a shows the XRD pattern of the as-deposited film of metallic tungsten (JCPDS 04-0806). After anodization, crystalline W was oxidized but the absence of any diffraction peaks in Fig. 1b reveals that the film transformed into amorphous tungsten oxide. The films became crystalline after annealing at 450, 500, and 550 °C, as shown by the sharp diffraction peaks of monoclinic tungsten trioxide (JCPDS 43-1035) in Fig. 1c, d, and e, respectively. The structure is similar to that reported in the literature [46]. It should be pointed out that although the same crystalline phase was observed, the intensity ratio between (002) and (200) peaks increased with increasing annealing temperature.

Fig. 2 shows the Raman spectra of WO_3 films annealed at 450, 500, and 550 °C, respectively (anodization time is 40 min). The spectra show the presence of very distinct Raman peaks at wave-numbers of 273, 328, 715, and 807 cm^{-1} for all annealed WO_3 films. The characteristic positions of these peaks are in agreement with the

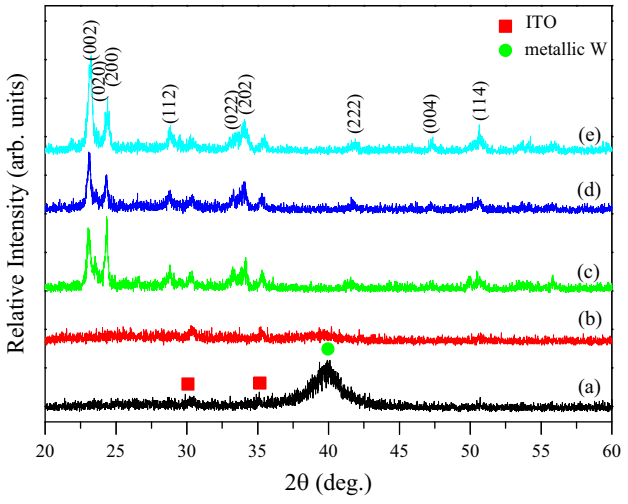

Fig. 1. XRD patterns of (a) as-deposited W film, (b) as-anodized WO_3 film, and WO_3 films anodized for 40 min and annealed at (c) 450, (d) 500, and (e) 550 °C.

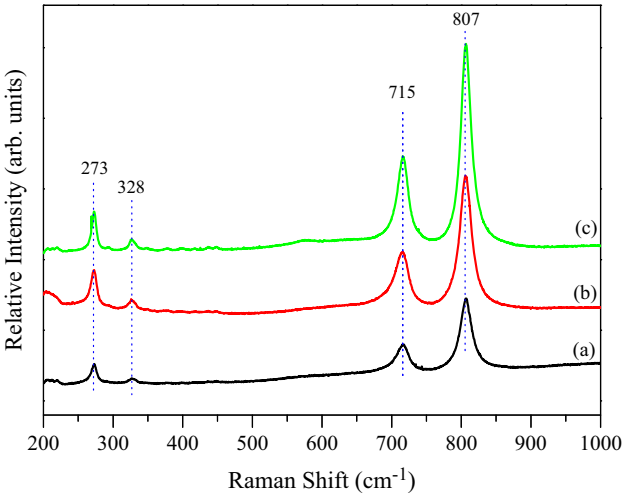

Fig. 2. Raman scattering spectra of WO_3 films anodized for 40 min and annealed at (a) 450, (b) 500, and (c) 550 °C.

fundamental mode of vibrations corresponding to the monoclinic phase of WO_3 [47]. A careful observation reveals that there is systematic increase in the intensity of the Raman peaks with increasing annealing temperature. This indicates that the crystallinity of WO_3 films was improved by annealing at higher temperature, which agrees well with XRD results.

Fig. 3 shows FE-SEM images of as-anodized and annealed WO_3 films. The W film after anodization has a porous microstructure (pore diameter $\sim$100 nm) formed by irregularly shaped grains. The thickness of the pore wall was estimated to be in the range of 40–80 nm. A similar wall size has been reported previously [8,41,43]. A significant change in the microstructure of WO_3 films was observed with increasing the annealing temperature. There was a gradual increase in the grain size and neck formation which may be attributed to the grain growth caused by sintering. The morphology of WO_3 films annealed at 450 °C (Fig. 3b) shows a porous microstructure with elongated grains. Similar microstructures were observed for all WO_3 samples annealed at 500 °C, as shown in Fig. 3c. The morphology of the WO_3 film annealed at 550 °C (Fig. 3d) shows a plate-like structure, which is due to the obvious sintering effect at higher annealing temperature.

The as-deposited tungsten film and as-anodized tungsten oxide films showed a poor electrochromic property. Fig. 4 shows the transmission spectra of WO_3 films annealed at 450, 500, and 550 °C, respectively (anodization time is 40 min). The solid and dotted lines represent the bleached and colored states, respectively. Optical modulation is the difference between the transmittance for bleached and colored films at 633 nm, and was estimated from the transmission spectra. The WO_3 film annealed at 500 °C had the largest optical modulation (43.6%) and that annealed at 550 °C had the lowest value (22.7%). The coloration efficiency (CE) is an important measure of the performance of electrochromic materials. It is calculated

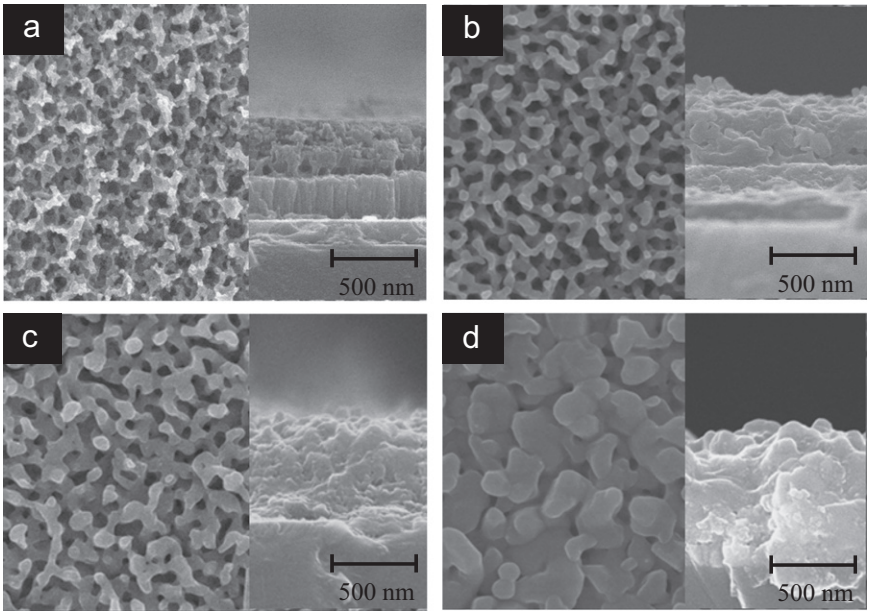

Fig. 3. SEM images of (a) as-anodized WO_3 films and films annealed at (b) 450, (c) 500, and (d) 550 °C (all samples were anodized for 40 min). Insets show the corresponding SEM cross-section images.

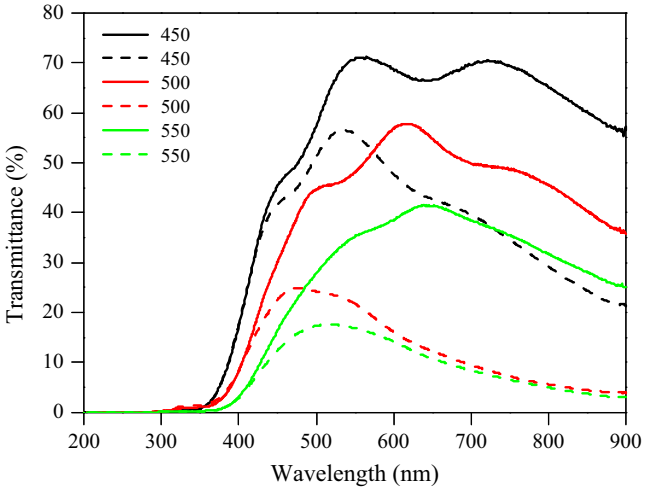

Fig. 4. Transmission spectra of bleached state (solid lines) and colored state (dashed lines) of WO_3 films anodized for 40 min and annealed at 450, 500, and 550 °C. Anodization time for all films was 40 min. (For interpretation of the references to color in this figure legend, the reader is referred to the web version of this article.)

by following equation [48],

$$CE(\eta) = \Delta OD(\lambda)/(q/A) = \log(T_b/T_c)/(q/A)$$

where T_b and T_c are the transmittance values of the WO_3 films in the bleached and colored states, respectively. The CE at a given wavelength is the variation of the optical density (ΔOD) for the charge (q) applied per unit electrode area (A). Table 1 shows the values of CE obtained for WO_3 films annealed at 450, 500, and 550 °C respectively. The film annealed at 500 °C shows the highest CE (42.8 $cm^2\,C^{-1}$). Generally, the electrochromic performance of tungsten oxide films is affected by several factors, including crystallinity, microstructure, and surface morphology. The as-anodized film was amorphous (Fig. 1a) and showed poor electrochromic performance, which was improved by post-annealing treatment. The enhancement of electrochromism for tungsten oxide films annealed at 450, 500, and 550 °C can be attributed to the improvement in crystallinity [47]. The surface morphology, however, was different due to the sintering effect. The structures, shown in Fig. 3b, c and d for WO_3 films are annealed at 450, 500, and 550 °C, respectively, influence the diffusion of Li^+ ions within the electrochromic material and thus affects the electrochromic property. The pore structure of the 500 °C-annealed WO_3 film exhibits the optimal pore network for the diffusion of Li^+ ions and possesses the superior electrochromic property.

In order to optimize the electrochromic performance the anodization time of WO_3 film was varied and the annealing temperature was fixed at 500 °C. The samples were characterized using XRD, SEM, refractive index, and Raman analysis. Fig. 5 shows the transmittance spectra at colored and bleached states for porous WO_3 films anodized for 20, 40, and 50 min, respectively, and annealed at 500 °C. The coloration efficiency and optical modulation were estimated. The results are listed in Table 1. The WO_3 film anodized for 40 min exhibited the best electrochromic performance, with a high optical modulation (ΔT_{633}—43.6%). This value is higher than those for WO_3 films anodized for 20 min (30.6%) and 50 min (28.5%). The coloration efficiency of the WO_3 film anodized for 40 min (42.8 $cm^2\,C^{-1}$) is significantly higher than those of films anodized for 20 min (31.5 $cm^2\,C^{-1}$) and 50 min (20.4 $cm^2\,C^{-1}$) even though these films have similar morphologies. Furthermore, the film relative density of WO_3 films, calculated by Lorentz–Lorenz formula is

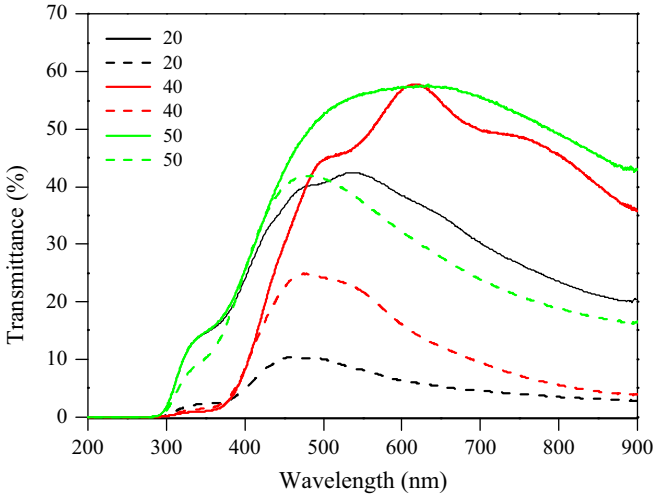

Fig. 5. Transmission spectra of bleached state (solid lines) and colored state (dashed lines) of WO_3 films annealed at 500 °C and anodized for 20, 40, and 50 min. (For interpretation of the references to color in this figure legend, the reader is referred to the web version of this article.)

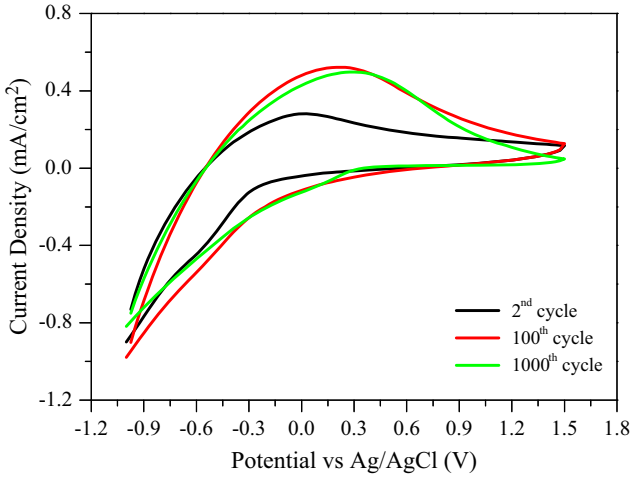

Fig. 6. Cyclic voltammograms of TO2 at the 2nd, 100th, and 1000th cycle.

shown in Table 1, decreases with the increase of anodization time as well as the decrease of annealing temperature. The relative density of TO2 shows the lowest value, 65.2%., as compared to TO4 and TO5, and may result in the difference of ΔT_{633}.

The stability of TO2 was examined by cyclic voltammetry (CV) tests for up to 1000 cycles in the applied voltage range of −1 to 1.5 V and Fig. 6 shows the results. It is noted that the TO2 exhibits the smallest loop area at the 2nd cyclic voltammograms that increased gradually with the increasing cycle number, reached its maximum at the 100th cycle, and decreased slightly thereafter. This indicates that the insertion of lithium ions may expose more active sites of the porous structure during cyclic voltammogram [49,50]. At the end of 1000 test cycles, the CV curve of TO2 did not show obvious variation. Only a slight decrease in the loop area and an anodic peak shift from 0.2 to 0.3 V was noticed.

4. Conclusion

Porous tungsten oxide films were prepared by the electrochemical anodization of RF-sputtered tungsten films. Annealed tungsten oxide films exhibited the monoclinic tungsten trioxide phase. The film morphology and crystallinity were influenced by the annealing temperature and porosity. The sintering effects include grain growth and neck formation. With increasing anodization time, the porosity of WO_3 film increased, but the crystallinity decreased. The WO_3 film anodized for 40 min and annealed at 500 °C exhibited the optimal pore structure for Li^+ ion diffusion and thus the best electrochromic performance.

Acknowledgments

The authors acknowledge the National Science Council of Taiwan for financial support of this research under Grant NSC 100-3113-E-006-004.

References

[1] W. Cheng, E. Baudrin, B. Dunn, J.I. Zink, Synthesis and electrochromic properties of mesoporous tungsten oxide, Journal of Materials Chemistry 11 (2001) 92–97.
[2] S.H. Baeck, K.S. Choi, T.F. Jaramillo, G.D. Stucky, E.W. McFarland, Enhancement of photocatalytic and electrochromic properties of electrochemically fabricated mesoporous WO_3 thin films, Advanced Materials 15 (2003) 1269–1273.
[3] C.G. Granqvist, electrochromic materials: out of a niche, Nature Materials 5 (2006) 89–90.
[4] S.H. Lee, R. Deshpande, P.A. Parilla, K.M. Jones, B. To, A.H. Mahan, A.C. Dillon, Crystalline WO_3 nanoparticles for highly improved electrochromic applications, Advanced Materials 18 (2006) 763–766.
[5] G.A. Niklasson, C.G. Granqvist, Electrochromics for smart windows: thin films of tungsten oxide and nickel oxide, and devices based on these, Journal of Materials Chemistry 17 (2007) 127–156.
[6] J. Zhang, J.P. Tu, X.H. Xia, Y. Qiao, Y. Lu, An all-solid-state electrochromic device based on NiO/WO_3 complementary structure and solid hybrid polyelectrolyte, Solar Energy Materials & Solar Cells 93 (2009) 1840–1845.
[7] Z.H. Jiao, X.W. Sun, J.M. Wang, L. Ke, H.V. Demir, Hydrothermally grown nanostructured WO_3 films and their electrochromic characteristics, Journal of Physics D: Applied Physics 43 (2010) 285501.
[8] J. Zhang, X.L. Wang, X.H. Xia, C.D. Gu, Z.J. Zhao, J.P. Tu, Enhanced electrochromic performance of macroporous WO_3 films formed by anodic oxidation of DC-sputtered tungsten layers, Electrochimica Acta 55 (2010) 6953–6958.
[9] J. Zhang, J.P. Tu, X.H. Xia, X.L. Wang, C.D. Gu, Hydrothermally synthesized WO_3 nanowire arrays with highly improved electrochromic performance, Journal of Materials Chemistry 21 (2011) 5492–5498.
[10] C.J. Schoot, J.J. Ponjee, H.T. Van-Dam, R.A. Van-Doorn, P.T. Bolwijn, New electrochromic memory display, Applied Physics Letters 23 (1973) 64–65.
[11] P. Bonhôte, E. Gogniat, F. Campus, L. Walder, M. Grätzel, Nanocrystalline electrochromic displays, Displays 20 (1999) 137–144.
[12] M.J. Wang, G.J. Fang, L.Y. Yuan, H.H. Huang, Z.H. Sun, N.H. Liu, S.H. Xia, X.Z. Zhao, High optical switching speed and flexible electrochromic display based on WO_3 nanoparticles with

ZnO nanorod arrays' supported electrode, Nanotechnology 20 (2009) 185304.
[13] C.M. Lampert, Toward large-area photovoltaic nanocells: experiences learned from smart window technology, Solar Energy Materials & Solar Cells 32 (1994) 307–321.
[14] C.G. Granqvist, Electrochromic oxides: systematics, materials, and applications to smart windows, Renewable Energy 5 (1994) 141–153.
[15] H. Yoshimura, N. Koshida, Fast electrochromic effect obtained from solid-state inorganic thin-film configuration with a carrier accumulation structure, Applied Physics Letters 88 (2006) 093509.
[16] A. Kraft, M. Rottmann, Properties, performance and current status of the laminated electrochromic glass of Gesimar, Solar Energy Materials & Solar Cells 93 (2009) 2088–2092.
[17] K. Bange, T. Gambke, Electrochromic materials for optical switching devices, Advanced Materials 2 (1990) 10–16.
[18] D. Ma, J. Jiang, J. Huang, D. Yang, P. Cai, L. Zhang, S. Huang, An unusual zinc substrate-induced self-construction route to various hierarchical architectures of hydrated tuingsten oxide, Chemical Communications 46 (2010) 4556–4558.
[19] L.F. Zhu, J.C. She, J.Y. Luo, S.Z. Deng, J. Chen, N.S. Xu, Study of physical and chemical processes of H_2 sensing of Pt-coated WO_3 nanowire films, Journal of Physical Chemistry C 114 (2010) 15504–15509.
[20] X. Zhang, X. Lu, Y. Shen, J. Han, L. Yuan, L. Gong, Z. Xu, X. Bai, M. Wei, Y. Tong, Y. Gao, J. Chen, J. Zhou, Z.L. Wang, Three-dimensional WO_3 nanostructures on carbon paper: photoelectrochemical properties and visible light driven photocatalysis, Chemical Communications 47 (2011) 5804–5806.
[21] M. Sadakane, K. Sasaki, H. Kunioku, B. Ohtani, R. Abe, W. Ueda, Preparation of 3-D ordered macroporous tungsten oxides and nanocrystalline particulate tungsten oxides using a colloidal crystal template method, and their structural characterization and application as photocatalysts under visible light irradiation, Journal of Materials Chemistry 20 (2010) 1811–1818.
[22] B.D. Alexander, P.J. Kulesza, L. Rutkowska, R. Solarska, J. Augustynski, Metal oxide photoanodes for solar hydrogen production, Journal of Materials Chemistry 18 (2008) 2298–2303.
[23] D.T. Gillaspie, R.C. Tenent, A.C. Dillon, Metal-oxide films for electrochromic applications: present technology and future directions, Journal of Materials Chemistry 20 (2010) 9585–9592.
[24] R.D. Rauh, Electrochromic windows: an overview, Electrochimica Acta 44 (1999) 3165–3176.
[25] C.G. Granqvist, Progress in electrochrmics: tungsten oxide revisited, Electrochimica Acta 44 (1999) 3005–3015.
[26] C.G. Granqvist, Electrochromic tungsten oxide films: review of progress 1993–1998, Solar Energy Materials & Solar Cells 60 (2000) 201–262.
[27] S.K. Deb, Opportunities and challenges in science and technology of WO_3 for electrochromic and related applications, Solar Energy Materials & Solar Cells 92 (2008) 245–258.
[28] J.M. Wang, E. Khoo, P.S. Lee, J. Ma, Controlled synthesis of WO_3 nanorods and their electrochromic properties in H_2SO_4 electrolyte, Journal of Physical Chemistry C 113 (2009) 9655–9658.
[29] C.G. Granqvist, E. Avendano, A. Azens, Electrochromic coatings and devices: survey of some recent advances, Thin Solid Films 442 (2003) 201–211.
[30] Y. Shen, T. Yamanzaki, Z. Liu, D. Meng, T. Kikuta, N. Nakatani, Influence of effective surface area on gas sensing properties of WO_3 sputtered thin films, Thin Solid Films 517 (2009) 2069–2072.
[31] A. Rougier, F. Portemer, A. Quéde', M. El Marssi, Characterization of pulsed laser deposited WO3 thins films for electrochromic devices, Applied Surface Science 153 (1999) 1–9.
[32] K.J. Patel, C.J. Panchal, M.S. Desai, P.K. Mehta, An investigation of the insertion of the cations H^+, Na^+, K^+ on the electrochromic properties of the thermally evaporated WO_3 thin films grown at different substrate temperatures, Materials Chemistry and Physics 124 (2010) 884–890.
[33] C.M. White, D.T. Gillaspie, E. Whitney, S.-H. Lee, A.C. Dillon, Flexible electrochromic devices based on crystalline WO_3 nanostructures produced with hot-wire chemical vapor deposition, Thin Solid Films 517 (2009) 3596–3599.
[34] W. Wang, Y. Pang, S.N.B. Hodgson, Design and fabrication of bimodal meso-mesoporous WO_3 thin films and their electrochromic properties, Journal of Materials Chemistry 20 (2010) 8591–8599.
[35] W. Cheng, E. Baudrin, B. Dunn, J.I. Zink, Synthesis and electrochromic properties of mesoporous tungsten oxide, Journal of Materials Chemistry 11 (2001) 92–97.
[36] S. Balaji, Y. Djaoued, A.-S. bastien Albert, R.Z. Ferguson, R. Brüning, Hexagonal tungsten oxide based electrochromic devices: spectroscopic evidence for the Li ion occupancy of four-coordinated square windows, Chemistry of Materials 21 (2009) 1381–1389.
[37] T. Brezesinski, D.F. Rohlfing, S. Sallard, M. Antonietti, B.M. Smarsly, Highly crystalline WO_3 thin films with ordered 3D mesoporosity and improved electrochromic performance, Small 2 (2006) (2006) 1203–1211.
[38] Z. Jiao, X. Wang, J. Wang, L. Ke, H.V. Demir, Tien Wei Koh, X.W. Sun, Efficient synthesis of plate-like crystalline hydrated tungsten trioxide thin films with highly improved electrochromic performance, Chemical Communications 48 (2012) 365–367.
[39] Z. Jiao, X.W. Sun, J. Wang, L. Ke, H.V. Demir, Hydrothermally grown nanostructured WO_3 films and their electrochromic characteristics, Journal of Physics D: Applied Physics 43 (2010) 285501.
[40] J. Yang, L. Jiao, Q. Zhao, Q. Wang, H. Gao, Q. Huan, W. Zheng, Y. Wang, H. Yuan, Facile preparation and electrochemical properties of hierarchical chrysanthemum-like WO_3 $0.33H_2O$, Journal of Materials Chemistry 22 (2012) 3699–3701.
[41] Y.C. Nah, A. Ghicov, D. Kim, P. Schmuki, Enhanced electrochromic properties of self-organized nanoporous WO_3, Electrochemistry Communications 10 (2008) 1777–1780.
[42] H. Zheng, A.Z. Sadek, K. Latham, K. Kalantar-Zadeh, Nanoporous WO_3 from anodized RF sputtered tungsten thin films, Electrochemistry Communications 11 (2009) 768–771.
[43] A. Watcharenwong, W. Chanmanee, N.R. de Tacconi, C.R. Chenthamarakshan, P. Kajitvichyanukul, K. Rajeshwar, Anodic growth of nanoporous WO_3 films: morphology, photoelectrochemical response and photocatalytic activity for methylene blue and hexavalent chrome conversion, Journal of Electroanalytical Chemistry 612 (2008) 112–120.
[44] K.M. Karuppasamy, A. Subrahmmanyam, Studies on the correlation between electrochromic colouration and the relative density of tungsten trioxide (WO_{3-x}) thin films prepared by electron beam evaporation, Journal of Physics D: Applied Physics 42 (2009) 095301.
[45] E. Washizu, A. Yamamoto, Y. Abe, M. Kawamura, K. Sasaki, Optical and electrochromic properties of RF reactively sputtered WO_3 films, Solid State Ionics 165 (2003) 175–180.
[46] C.L. Wu, C.K. Wang, C.K. Lin, S.C. Wang, J.L. Huang, Electrochromic properties of nanostructured tungsten oxide films prepared by surfactant-assistedsol–gel process, Surface and Coatings Technology, http://dx.doi.org/10.1016/j.surfcoat.2012.01.061.
[47] C. Santato, M. Odziemkowski, M. Ulmannn, J. Augustynski, Crystallographically oriented mesoporous WO_3 films: synthesis, characterization, and applications, Journal of the American Chemical Society 123 (2001) 10639–10649.
[48] C.G. Granqvist, in: C.G. Granqvist (Ed.), Renewable Energy Series: Materials Science for Solar Energy Conversion Systems, Pergamon Press, Oxford, UK, 1991.
[49] C.O. Avellaneda, P.R. Bueno, R.C. Faria, L.O.S. Bulhoes, Electrochromic properties of lithium doped WO_3 films prepared by the sol–gel process, Electrochimica Acta 46 (2001) 1977–1981.
[50] M. Deepa, T.K. Saxena, D.P. Singh, K.N. Sood, S.A. Agnihotry, Spin coated versus dip coated electrochromic tungsten oxide films: structure, morphology, optical and electrochromic properties, Electrochimica Acta 51 (2006) 1974–1989.